

Numerical Simulation of Interaction between Two Wind Turbines of Vertical Axis

Kanako Ikeda, Anna Kuwana, Yusaku Nagata, and Tetuya Kawamura

(Received: 26th December 2016)

Abstract

Two-dimensional flow around two straight wing vertical axis wind turbines (SW-VAWT) with two blades is investigated by means of the numerical simulation. Special attention is paid for the interaction between two wind turbines. It is desired to use rotational coordinate system in order to perform precise computations. Therefore, we divide whole computational domain into several sub-domains two of which rotate around the axis of each wind turbine. These sub-domains are embedded in outer motionless domain. Incompressible Navier-Stokes equations are solved by the fractional step method. The third order upwind difference is chosen for the approximation of non-linear terms. Torque coefficients of two wind turbines are computed changing tip speed ratio to see the interaction between them.

1 Introduction

In recent years, wind farm has much attention as a ‘zero-emission’ natural energy source. On the other hand, there are not enough suitable places for constructing wind turbines. As a result, many wind turbines are located closely and the interaction between wind turbines cannot be ignored.

The straight wing vertical axis wind turbine (SW-VAWT) is suitable for wind farm because this turbine rotates at an appropriate speed for power generation by wind in any direction (Figure 1). In many studies about the SW-VAWT [1-7], performance of single turbine has been investigated but not in the case of many turbines. In numerical simulations, a rotational coordinate system rotating with a turbine can be used to calculate the single turbine [7-9], however such a simple method cannot be used in the case of many turbines.

In this study, we focus on the two-dimensional SW-VAWT and investigate the interaction between two wind turbines. We use the overset grid that consists of two rotational coordinates for each turbine immersed in a steady coordinate to calculate this turbines’ system.

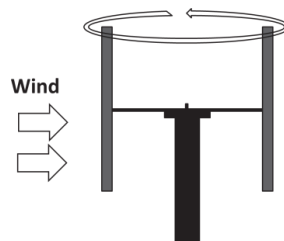


Figure 1 Example of straight wing vertical axis wind turbine (SW-VAWT)
with two blades

2 Numerical method

2.1 Basic equations

We use the equations of continuity and the incompressible Navier-Stokes equations as governing equations on both the steady coordinate system and the rotational coordinate system. On the rotational coordinate system, they are expressed as follows:

$$\frac{\partial U}{\partial X} + \frac{\partial V}{\partial Y} = 0$$

$$\frac{\partial U}{\partial t} + U \frac{\partial U}{\partial X} + V \frac{\partial U}{\partial Y} - \omega^2 X + 2\omega V = -\frac{\partial p}{\partial X} + \frac{1}{Re} \left(\frac{\partial^2 U}{\partial X^2} + \frac{\partial^2 U}{\partial Y^2} \right)$$

$$\frac{\partial V}{\partial t} + U \frac{\partial V}{\partial X} + V \frac{\partial V}{\partial Y} - \omega^2 Y - 2\omega U = -\frac{\partial p}{\partial Y} + \frac{1}{Re} \left(\frac{\partial^2 V}{\partial X^2} + \frac{\partial^2 V}{\partial Y^2} \right)$$

where X , Y and U , V are the position and velocity components on the rotational coordinate system and ω is the angular velocity, respectively. There are following relations between the steady coordinate system and the rotational one:

$$x = X \cos \theta + Y \sin \theta$$

$$y = -X \sin \theta + Y \cos \theta$$

$$X = x \cos \theta - y \sin \theta$$

$$Y = x \sin \theta + y \cos \theta$$

Also relations of velocity components between two coordinate systems are as follows:

$$u = U \cos \theta + V \sin \theta + \omega y$$

$$v = -U \sin \theta + V \cos \theta - \omega x$$

$$U = u \cos \theta - v \sin \theta - \omega Y$$

$$V = u \sin \theta + v \cos \theta + \omega X$$

where x , y and u , v are the position and velocity components on the steady coordinate systems and θ is the rotation angle. Schematic figure of two coordinate systems is shown in Figure 2.

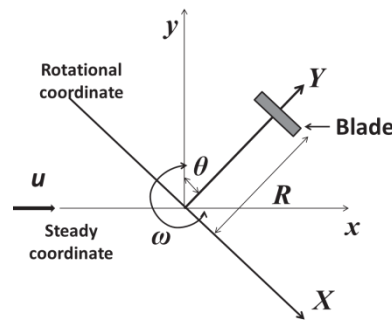


Figure 2 Two coordinate systems

2.2 Finite differential solutions

The governing equations are solved numerically by the fractional step method.

In order to solve them stably even at high Reynolds number, non-linear terms are approximated by the third order upwind finite differential method. All the spatial derivatives except for non-linear terms are approximated by the second order central difference method.

2.3 Layout of wind turbine

We simulate the flow field around two rotating SW-VAWTs with two blades. Figure 3 shows schematic diagram of two wind turbines. We assume that they are the same size and the same shape and rotate with the same phase in the uniform wind of tandem direction as the test case although these assumptions are not necessary in the numerical method proposed in this study.

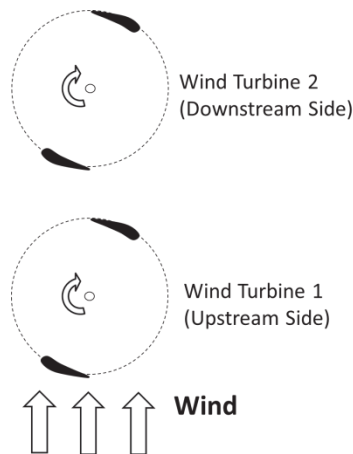


Figure 3 Schematic diagram of two wind turbines

2.4 Grid systems

The grids are generated separately in two regions each of which includes one wind turbine as shown in Figure 4. They are connected along one side CD in the figure.

Each region has two sub-regions A and B. The region A rotates together with the wind turbine and the region B is fixed in the space. The outer boundary of A and inner boundary of B is “overlapped circle” so that it is easy to transfer the flow data of one region into another region through the interpolation.

In region A, O-type grid system is chosen because it is not sensitive to the flow direction that is changing according to the rotation of the wind turbine. For the accuracy of the calculation, the grids are concentrated near the blades.

The outer edge of region B is rectangle that has one straight side CD mentioned above. The total number of grid points in each region is 121×69 .

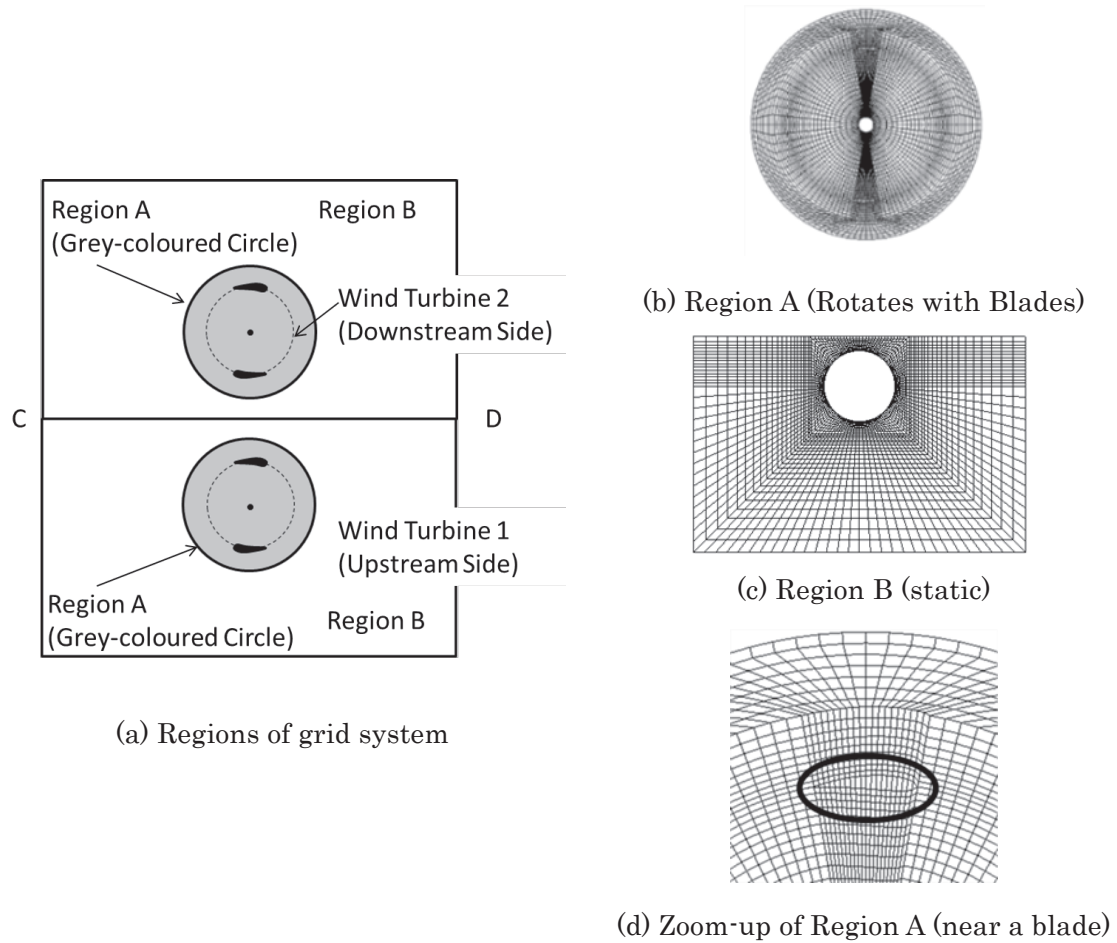


Figure 4 Grid systems

2.5 Boundary condition

Two wind turbines are assumed to rotate with the same angular velocity. No-slip condition is imposed on the blades. On the far boundary, the flow is assumed to be uniform.

2.6 Calculation condition

In order to estimate the performance of the wind turbine, we change tip speed ratio λ defined by the following formula:

$$\lambda = \frac{\omega R}{V_{\infty}} \quad R: \text{radius of wind turbine}, \quad V_{\infty}: \text{wind speed}$$

The radius of wind turbine i.e. half distance between blades is 2.8 times as long as the chord length. Two wind turbines are settled apart from distance of 4 times as long as the radius of the wind turbine. By setting the parameter $\lambda = 2, 4$ and 6 , we calculate the flow. The Reynolds number based on the uniform flow and the cord length is 2,000.

3 Results and Discussions

To see the interaction between two wind turbines, two cases (case 1 and case 2) are computed and compared. In case 1, wind turbine of upwind side is rotating and that of downwind is stopped. Since the flow of this case is similar to the flow around only one wind turbine, we call it the case of single turbine. The results of this case are denoted by Figures 5-10 (a) below. In case 2, two wind turbines are rotating with the same speed and the results are shown in Figures 5-10 (b).

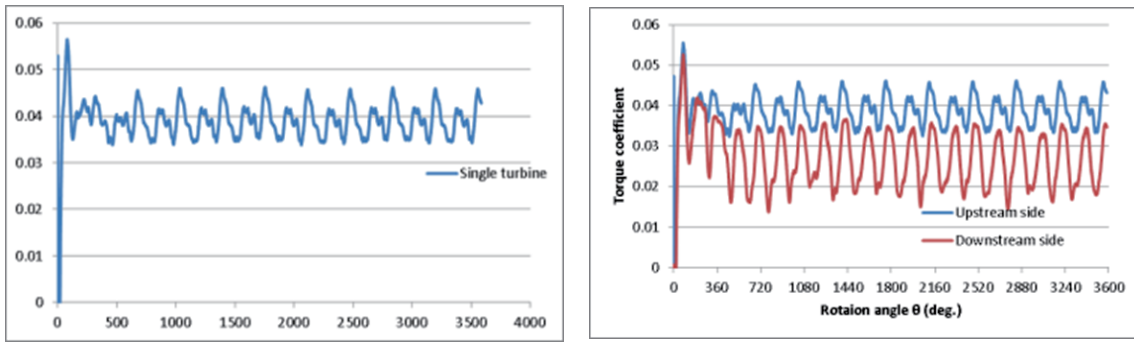
3.1 Torque

Figure 5, 6 and 7 show the relationship between rotation angle and torque coefficient for $\lambda = 2, 4, 6$. In each figure, a blue curve shows upstream side and a red curve shows downstream side. Since each line near the origin is in unsteady state, we focus on the part except for this region.

For $\lambda = 2$, the curve in Figure 5 (a) and that of the blue curve in Figure 5 (b) are almost the same. This shows that the downstream turbine does not have an impact on the upstream turbine. On the other hand, the upstream turbine affects greatly on the downstream turbine so that the mean torque coefficient of the downstream one decrease up to about 2/3 of the upstream one. Also, the amplitude of oscillation of downstream turbine is much smaller than that of the upstream turbine.

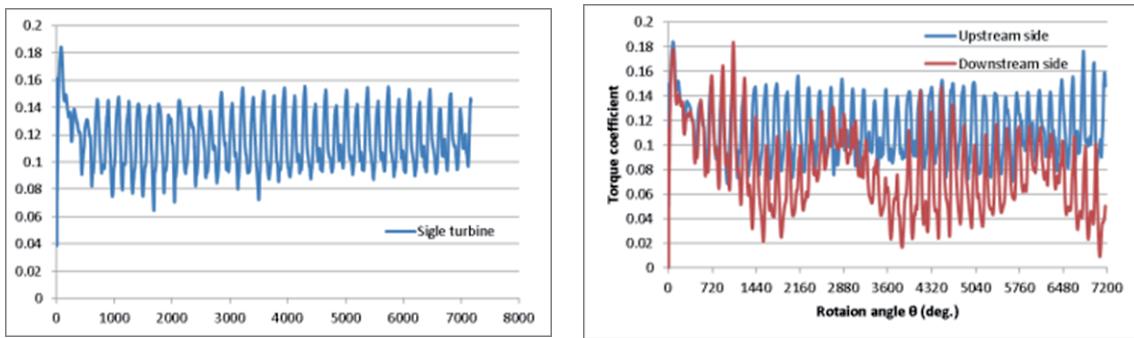
The results for $\lambda = 4$ are similar to those for $\lambda = 2$ as are shown in Figure 6 and Figure 5. The upstream turbine is a little bit influenced by the downstream turbine. This tendency is also seen in Table 1 that tabulates mean torque coefficients. On the other hand, the downstream turbine is influenced greatly by the upstream turbine. In this case, the torque coefficient is about 2/3 of the upstream turbine. In addition, the torque coefficient of the downstream turbine oscillates largely except for 180 degrees. The torque coefficient for $\lambda = 4$ is three times as large as that for $\lambda = 2$.

In the case of $\lambda = 6$, all curves are quite different. However, the torque coefficients of the upstream turbine and the downstream turbine are almost the same as that of single turbine. They are five times as large as in the case of $\lambda = 2$. Although it is difficult to find out rational reasons, it seems that the assumption that two turbines rotate at the same fixed speed is not realistic.



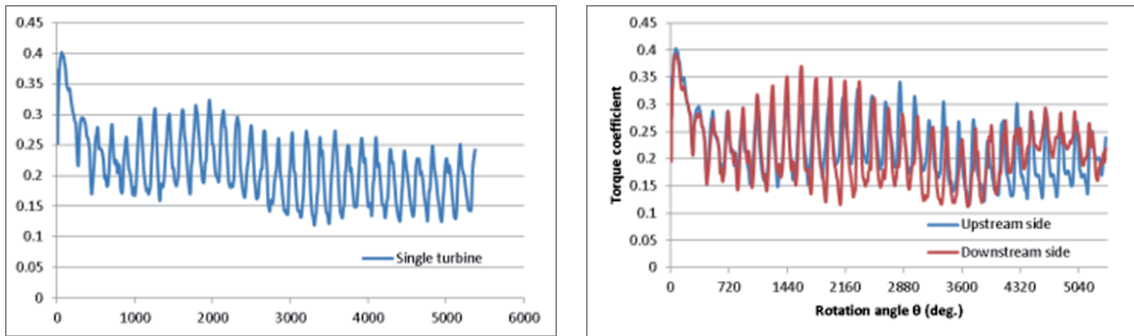
(a) Single turbine (b) Two turbines

Figure 5 Time history of torque coefficient $\lambda = 2$



(a) Single turbine (b) Two turbines

Figure 6 Time history of torque coefficient $\lambda = 4$



(a) Single turbine (b) Two turbines

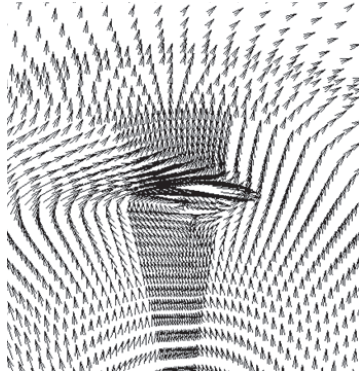
Figure 7 Time history of torque coefficient $\lambda = 6$

Table 1 Mean torque coefficient

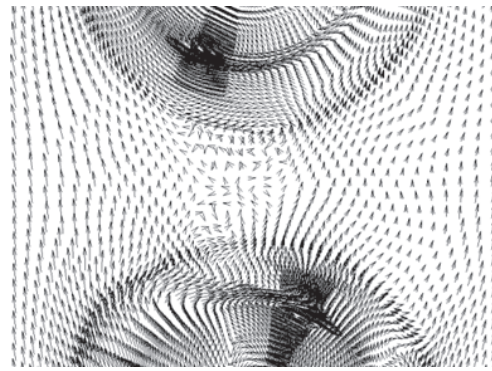
	$\lambda = 2$	$\lambda = 4$	$\lambda = 6$
Single turbine	0.0390	0.1151	0.1974
Two turbines (Upstream side)	0.0389	0.1120	0.2102
Two turbines (Downstream side)	0.0265	0.0730	0.2065

3.2 Velocity field

Figure 8, 9 and 10 show the snapshots of velocity field near the blade for $\lambda = 2, 4$ and 6 . In the case of single turbine, these figures are drawn when the angle between the blade and uniform flow becomes right angle. In the case of two turbines, they are drawn at the moment just after the distance between the blades of each turbine becomes the shortest.

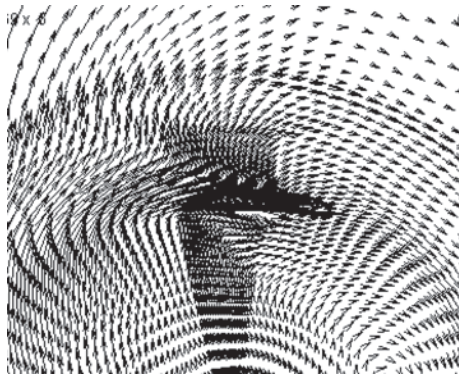


(a) Single turbine $\theta = 720$ degrees

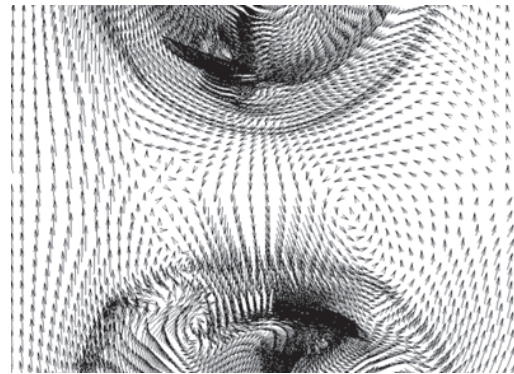


(b) Two turbines $\theta = 3460$ degrees

Figure 8 Velocity vector $\lambda = 2$



(a) Single turbine $\theta = 720$ degrees

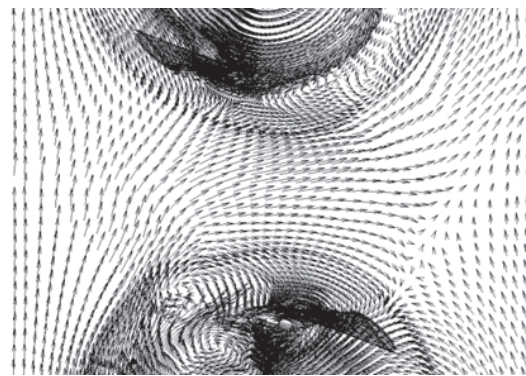


(b) Two turbines $\theta = 7070$ degrees

Figure 9 Velocity vector $\lambda = 4$



(a) Single turbine $\theta = 720$ degrees



(b) Two turbines $\theta = 5260$ degrees

Figure 10 Velocity vector $\lambda = 6$

In the case of two turbines for $\lambda = 2$, the flow near the rear turbine becomes weak due to the effect of the front turbine as is shown in Figure 8 (b). In the case of two turbines for $\lambda = 4$, we can find asymmetric vortices behind the front turbine. These vortices are generated by the front turbine rotating rapidly as if a rotating cylinder of radius R exists in front of the rear turbine.

In the case of two turbines for $\lambda = 6$, we can find a strong stream flowing from left to right between blades of each wind turbine. Due to this stream, the torque coefficient of the rear wind turbine becomes larger than expected.

4 Conclusion

The flow around the two SW-VAWTs with two blades is simulated in order to find out the interaction between two wind turbines. Special attention is paid for the torque coefficient of two turbines and the velocity field near the blades of turbines. Tip speed ratio λ is changed in three ways, i.e. 2, 4 and 6.

For $\lambda = 2$, the downstream turbine does not have an impact on the upstream turbine. On the other hand, the upstream turbine affects greatly on the downstream turbine.

For $\lambda = 4$, the upstream turbine is a little bit influenced by the downstream turbine, while the downstream turbine is influenced greatly by the upstream turbine. The torque coefficient for $\lambda = 4$ is three times as large as that for $\lambda = 2$.

For $\lambda = 6$, the torque coefficients of the upstream turbine and the downstream turbine are almost the same as that of single turbine. This is perhaps due to a strong stream between two turbines. The coefficients are five times as large as in the case of $\lambda = 2$.

In the future, we increase the number of grid points around blades in order to calculate with high accuracy and make a three-dimensional model.

References

- [1] K. Ishimatsu, K. Kage and T. Okubayashi, "Numerical Simulation for Flow Fields of Darrieus Turbine", Transactions of the JSME(B), No.61, Vol.587, (1995), pp.2543-2548.
- [2] I. Paraschivoiu, "Wind Turbine Design: With Emphasis on Darrieus Concept", Presses inter Polytechnique, (2002).
- [3] K. Horiuchi, I. Ushiyama and K. Seki, "Straight Wing Vertical Axis Wind Turbines: A Flow Analysis", Wind Engineering, Vol.29, No.3, (2005), pp.243-252.
- [4] Y. Sato, H. Okazaki, T. Shoda, Y. Nishio, M. Shigeta, S. Izawa, "Hotwire Measurement and Numerical Analysis of Flows around a Straight Wing Vertical Axis Wind Turbine", Transactions of the JSME(B), No.77, Vol.775, (2011), pp.637-646.
- [5] H. J. Sutherland, D. E. Berg and T. D. Ashwill, "A Retrospective of VAWT Technology", Sandia Report, (2012).
- [6] C. Anagnostopoulou, H. Kagamoto, K. Sao and A. Mizuno, "Concept Design and Dynamic Analyses of a Floating Vertical-Axis Wind Turbine: Case Study of Power Supply to Offshore Greek Islands", Journal of Ocean Engineering and Marine Energy, Vol.2, Issue 1, (2016), pp.85-104.

- [7] Y. Mizukami, and T. Kawamura, "Numerical study of the performance of straight-wing vertical-axis-wind-turbine with two and three blades", Natural Science Report, Ochanomizu University, Vol.59, No.2, (2009), pp.47-54.
- [8] A. Kuwana, Y. Sato, and T. Kawamura, "Numerical Simulation of the Performance of Modified Savonius Rotors for the Purpose of Pumping Water", CFD Journal, Vol.15, No.4, (2007), pp.598-602.
- [9] Y. Yoshida, and T. Kawamura, "Numerical simulations of two-dimensional flows around a Savonius rotor with various curvature of the blade", Natural Science Report of the Ochanomizu University, Vol.63, No.1, (2012), pp.11-21.

Kanako Ikeda
Ochanomizu University
2-1-1 Otsuka, Bukyo-ku, Tokyo, 112-8610, Japan
Email: ikeda.kanako@is.ocha.ac.jp

Anna Kuwana
Email: kuwana.anna@ocha.ac.jp

Yusaku Nagata
Email: nagata.yusaku@is.ocha.ac.jp

Tetuya Kawamura
Email: kawamura@is.ocha.ac.jp